Pervasive effects of drought on tree growth across a wide climatic gradient in the temperate forests of the Caucasus

Article *in* Global Ecology and Biogeography · September 2018
DOI: 10.1111/geb.12799

7 authors, including:

Darío Martín-Benito
Instituto Nacional de Investigación y Tecnología Agraria y Alimentaria

Neil Pederson
Harvard University

Nesibe Köse
Istanbul University

Mehmet Doğan
Ege University

Supporting Information

Pervasive effects of drought on tree growth across a wide climatic gradient in the temperate forests of the Caucasus

Global Ecology and Biogeography. DOI:10.1111/geb.12799

Dario Martin-Benito [1,2,3], Neil Pederson[4], Nesibe Köse[5], Mehmet Doğan[6], Harald Bugmann[2], Marine Mosulishvili[7,8], Christof Bigler[2]

Affiliations
1, Forest Research Center INIA-CIFOR, Ctra. La Coruña km. 7.5, 28040 Madrid, Spain
2, Forest Ecology, Institute of Terrestrial Ecosystems, Department of Environmental Systems Science, ETH Zurich, Universitätstrasse 22, 8092 Zurich, Switzerland
3, Tree Ring Laboratory of Lamont Doherty Earth Observatory, Columbia University, 61 Rt 9W, Palisades, NY 10976, United States
4, Harvard Forest, Harvard University, 324 North Main St., Petersham, Massachusetts 01366, United States
5, Faculty of Forestry, Forest Botany Department, Istanbul University, 34473 Bahçeköy-Istanbul, Turkey
6, Ege University, Faculty of Letters, Department of Geography, Bornova, Izmir, Turkey
7, Institute of Ecology, Ilia State University; Cholokashvili Ave. 3/5, Tbilisi 0162, Georgia.
8, Georgian National Museum, Purtseladze St. 3, Tbilisi 0105, Georgia

Date: 23 April 2018

Contents

Supplementary methods

Regional climate.

Climate in the Caucasus region is affected by i) different atmospheric circulation patterns, ii) the presence of two large bodies of water to the east and west and, iii) the rough topography of its mountains. During most of the year the area experiences a strong influence of westerly winds that bring moisture from the Black Sea (Stanev & Rachev, 1999). These moist air masses are forced to rise by the presence of mountains over 3000 m a.s.l. in elevation causing local to regional orographic precipitation added to more regional cyclonic precipitation. These two effects combined create large precipitation gradients with some areas facing the Black Sea receiving over 3000 mm·year^{-1}, while others in rain-shadows receive less than 500 mm·year^{-1} (Figure S1 and Figure S2). In addition to this local or regional influences, the region is also affected by more remote influences from general circulation patterns although these effects might be lagged (Zveryaev, 2004; Martin-Benito, Ummenhofer, Köse, Güner & Pederson, 2016). During the winter and spring, precipitation in the Caucasus is affected by the North Atlantic Oscillation (NAO) similarly to other regions to the west such as central Anatolia, the Middle East and the Mediterranean Basin (Cullen & Demenocal, 2000; Martin-Benito et al., 2016; Türkeş & Erlat, 2003). The area is also affected by two anticyclones centered in western Russia during the winter and spring and a second one centered over Scandinavia and Western Europe during the spring (Golubev, Kuftarkov & Golubeva, 1993). Despite the large absolute differences in climate between different parts of the region, the common interannual variability is high for precipitation, temperature and drought (Figure S3). The Caucasus region is considered to have some of the largest amounts of precipitation in Europe but also to experience higher interannual variability (Zveryaev, 2004).

Precipitation differences across the region are lowest during spring because in general spring is the driest season for the wetter areas, while it is the wettest season for the drier areas (Figure S1) (Martin-Benito et al., 2016). See for example the Walter climate diagram for grid points 3 (driest) and 11 (wettest) in Figure S2. Because spring is the most influential season in terms of precipitation, it either represents the most limiting period in terms of soil moisture for the wet areas or the time when soil moisture is recharged for the dry areas.

Our network includes sites (Figure S2 and Table S2) across a wide climate gradient from wet and warm sites such as AJA, KUT or KEDA to cold and dry sites such as TURK009 or wet and cold sites such as KINH and KINM. It is worth noting that because climate data is scarce in the area and we had to use gridded climate products, the real climate gradients are certainly larger than what gridded products show. Also, the *P. pinea* site (HAT) in the Upper Coruh River Basin (Table S1) is the only site that experiences a Mediterranean climate (Csb, warm, dry summers and wet cold seasons) in our network but its unique climate is not completely captured by gridded climate data.

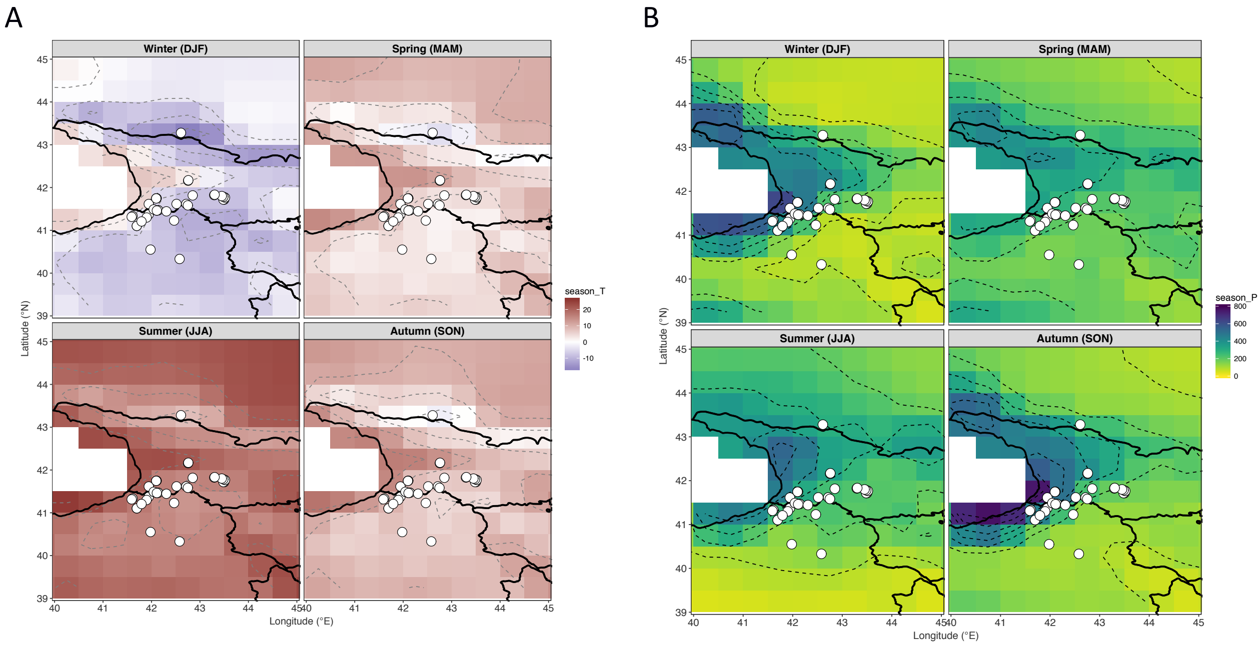

Figure S1.
Summary seasonal climatology in the Caucasus region for 1930-2009 from two gridded data sets: A, temperature from CRU_TS4.01 (Harris, Jones, Osborn & Lister, 2014); right, precipitation from GPCC v5 (Rudolf, Becker, Schneider, Meyer-Christoffer & Ziese, 2011).

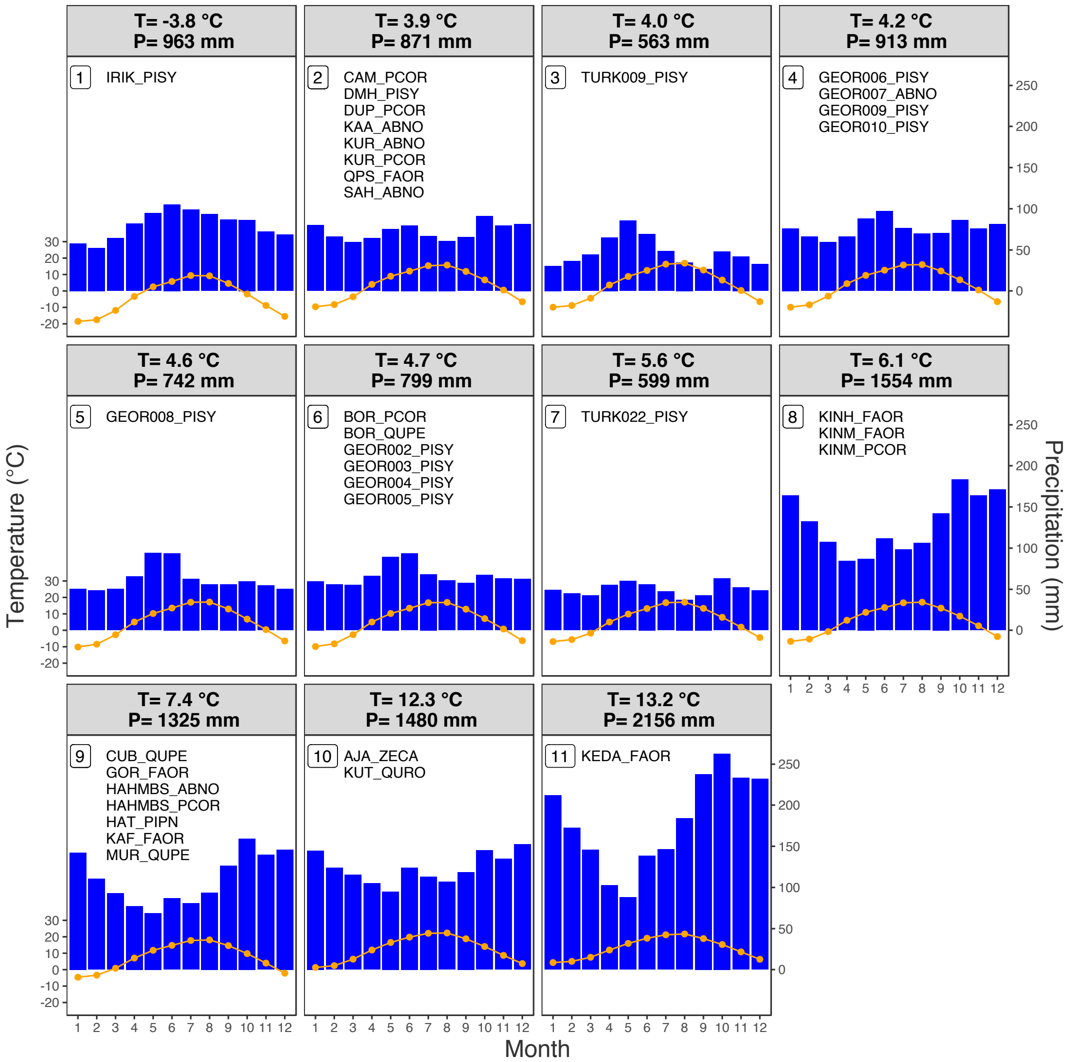

Figure S2.
Walter climate diagrams for each grid-point (1930-2009) from two gridded data sets: blue bars for GPCC v5 precipitation (Rudolf et al., 2011); and orange lines for CRU_TS4.01 temperature (Harris et al., 2014). On top of each panel, mean annual temperature and mean total precipitation are shown. Chronologies for which that grid-point is the closest are shown in each panel (see Table S2). Panel numbering is used in Figure S3. Codes refer to sites and species (see Figure 1).

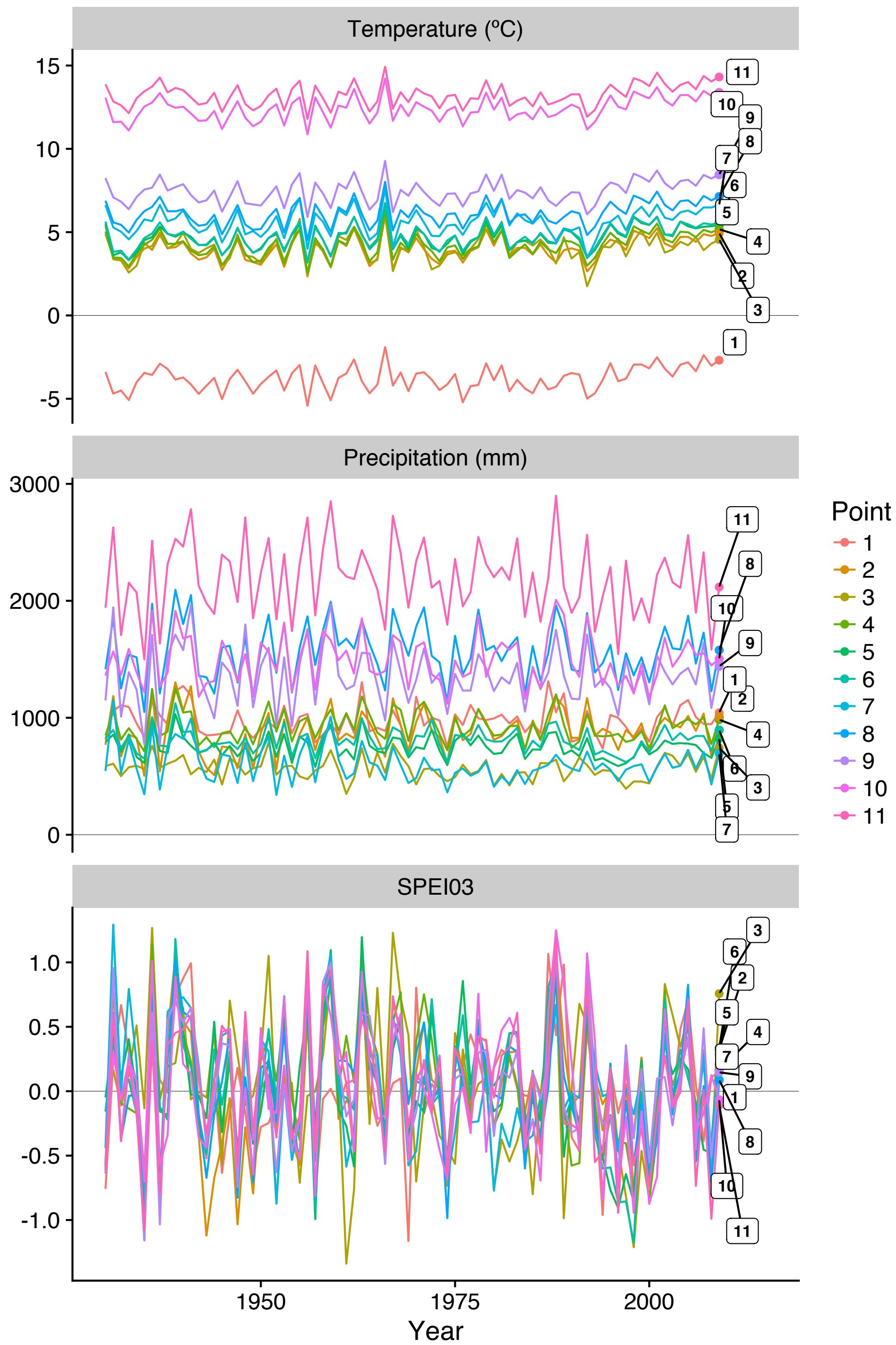

Figure S3.
Climate time series for each grid-point (1930-2009) from two gridded data sets: GPCC v5 for precipitation (Rudolf et al., 2011); and CRU_TS4.01 for temperature (Harris et al., 2014). SPEI03 is estimated from precipitation and temperature (Vicente-Serrano, Beguería & López-Moreno, 2010). Grid point numbers correspond to panel numbers in Figure S2.

Regional vegetation.

The Caucasus lies between two different phytogeographical regions: the Euxinian province of the Euro-Siberian region, and the Hyrcanian province of the Irano-Turanian region (Dellasala, 2011; Browicz, 1989). Thus, the region shares some common genera with central European temperate forests, but also hosts Arcto-Tertiary relicts (e.g., *Zelkova*, *Pterocarya*) (Dellasala, 2011). The region shares some genera with central European temperate forests (e.g., *Fagus*, *Quercus*, *Abies* and *Picea*), but it also hosts Arcto-Tertiary relicts (e.g., *Zelkova*, *Pterocarya*) (Dellasala, 2011). Because of the large and abrupt climatic differences and the rough topography (Figure S1), vegetation transitions from temperate rainforests dominated by broadleaf genera (*Alnus*, *Fagus, Castanea*), with a dense, tall evergreen understory (e.g. *Rhododendron* spp.) in the western wetter areas, to the dark conifer forests (dominated by *Abies*, *Picea*, *Pinus*) at drier and continental neighboring areas to the east and south, to the treeless steppe in the most arid areas (Browicz, 1989). The Colchic rainforest is restricted to the wetter areas of the mountains and piedmont bordering the Black Sea, the dominant species of these rainforests (*Fagus*, *Picea*, *Castanea*) extend beyond these wetter areas which creates a good opportunity to study them along important climate gradients and explore the role of climate and future climate changes in their growth and ecology (Table S1).

Our network included a of a total of 35 sites from four broadleaved species [*Quercus petraea* (Matt.) Liebl., *Quercus robur* L., *Fagus orientalis* Lipsky, and *Zelkova carpinifolia* (Pall.) K. Koch.] and four conifer species [*Abies nordmanniana* (Steven) Spach, *Pinus sylvestris* L., *Picea orientalis* L., and *Pinus pinea* L.] (Table S2). Some of these species have a Europe-wide distribution like *P. sylvestris* (Scots pine), *Q petraea* (Sessile oak) and *Q. robur* (European oak). Other species have distribution ranges limited to the south and eastern border of the Black Sea, such as *P. orientalis* (eastern spruce), *F. orientalis* (eastern beech) and *A. nordmanniana* (Caucasian fir). This network also includes the relict endemic species *Z. carpinifolia* (Caucasian elm) and a rare population of the Mediterranean *P. pinea* (Stone pine). Because sweet chestnut (*Castanea sativa*) in the area has been decimated by chestnut blight (*Cryphonectria parasitica* (Murr.) Barr.) across much of its distribution area including the Caucasus (Daniel & Simone, 2018), this species was not included in our tree ring network.

Fagus orientalis is a shade tolerant species (Fleck, Niinemets, Cescatti & Tenhunen, 2003) of medium drought sensitivity (Niinemets & Valladares, 2006) that dominates areas with high moisture availability from 500 m to 2000 m a.s.l. (timber line), mainly in the windward side of the mountains facing the Black Sea. In these wet forests, *P. orientalis* and *A. nordmanniana* (collectively known as dark coniferous) appear mainly in forest gaps or disturbed areas but their dominance increases towards relatively dryer and colder areas in the interior dark coniferous forests as *F. orientalis* presence decreases. These two conifers, however, are sometimes classified as more drought sensitive and shade tolerant than *F. orientalis* (Niinemets & Valladares, 2006). *Pinus sylvestris* is a more drought tolerant and less shade tolerant species that can appear in dry slopes at almost any altitude above 800 m a.s.l. (although it exceptionally reaches sea level near Rize, Turkey) and may dominate at dry and cold sites. As the most drought tolerant species in our network, *Quercus petraea* is found at mid elevation on south-facing, rocky slopes where it forms mixed forests with *Castanea sativa*, *F. orientalis*, *P. sylvestris* or *P. orientalis*. Populations of *Q. petraea* in eastern Anatolia are sometimes considered to be a *Q. petraea subsp. iberica* or the different species *Quercus iberica Steven ex M. Bieb.) (Papini, Simeone, Bellarosa, Spada & Schirone, 2011). Zelkova carpinifolia* is a hygro-thermophilous, light-demanding species almost exclusively restricted to the Caucasus region and Northern Iran with some of its largest populations found in the Colchic lowlands of western Georgia (Kvavadze & Connor, 2005; Kozlowski & Gratzfeld, 2013). In this same area of deep and moist alluvial soils, the drought tolerant and light demanding *Quercus robur* has its only south Caucasian populations which are sometimes considered to be a different sub-species *Quercus robur* L. subsp. *imeretina* (Steven ex Woronow) Menitsky. Similar to other parts of western Eurasia, however, the species distribution in the Caucasus is not only dependent on current climate and it is largely influenced by refugia during the last glacial maximum and later recolonization (Tarkhnishvili, Gavashelishvili & Mumladze, 2012), so potential distribution areas are probably much larger than currently realized areas.

Table S1. Main forest types in our dendrochronological network*

Zone	Forest type/zone	Vegetation [a]	Elevation (m a.s.l.)	Climate [b]	Sites in network [d]
West Caucasian (Colchic)	Humid thermophilous Colchic broad-leaved forest	***Zelkova carpinifolia, Quercus robur***, *Fagus orientalis*	0-1000	Cfa	AJA, KUT
	Beech-chestnut forests with oak and Colchic underwood [c]	***Fagus orientalis, Quercus petraea***, *Castanea sativa*	500-1200	Cfb	KEDA, MUR, CUB
	Humid beech forest zone [c]	***Fagus orientalis, Picea orientalis, Abies nordmanniana***, *Quercus pontica*	800-1800	Cfb - Cfa	QPS, GOR, CAM, KINH, KINM, DUP, KAA, KUR, KAF
	Nemoral humid coniferous forest [c]	***Picea orientalis, Abies nordmanniana***, *Fagus orientalis*	1400-2100	Cfb - Cfa	DUP, SAH, HAH, BOR, KUR
	Subalpine conifer forest	***Pinus sylvestris, Abies nordmanniana***	1700-2200	Dfb	DMH, GEOR007
	Mediterranean	***Pinus pinea***	Upper Choruh River Basin	Csb	HAT
East Caucasian	Lower mountain belt	***Quercus petraea***	500-1000	Cfa-Cfb	BOR
	Middle mountain belt	***Picea orientalis, Pinus sylvestris***, *Fagus orientalis*	1000-1500	Dfb	BOR, GEOR004, GEOR005
	Upper mountain belt	***Picea orientalis, Pinus sylvestris***, *Fagus orientalis*	1500-2000	Dfa-Dfb	GEOR002, GEOR003, GEOR006, GEOR008, GEOR009, GEOR0010
	Lower subalpine belt	***Pinus sylvestris***		Dfb-Dfc	IRIK
South Caucasian	Hemi-xeric woodland	***Pinus sylvestris***	1600-2400	Dfa-Dfb	TURK009, TURK022

*, Based on Zazanashvili, Gagnidze and Nakhutsrishvili (2000); Zazanashvili (1999); Browicz (1989)
a, names in bold denote species included in our network for that zone and vegetation type
b, Köppen climate: Cfa, warm temperate, fully humid climate with hot summers; Cfb, warm temperate, fully humid with warm summers; Csb, temperate with dry, warm summer (Mediterranean); Dfb, snowy climate, fully humid with warm summers; Dfc, Snowy climate, fully humid with cool summers (Kottek, Grieser, Beck, Rudolf & Rubel, 2006).
c, these forest types may include temperature rainforests.
d, for site information see Table S2.

Table S2. Summary information on tree-ring sites in the network

Site	Species	Number of Cores/ trees	Latitude (N)	Longi tude (E)	Elevation (m.a.s.l)	Country	Site characteristics	Source[a]
KUR	ABNO	24/21	41.47º	42.14º	2075	Turkey	Managed forest	this work
SAH	ABNO	36/22	41.23º	42.47º	2000-2100	Turkey	Managed forest	this work
GEOR007	ABNO	27/13	41.62º	42.52º	1930	Georgia	na	ITRDB
HAH	ABNO	13/12	41.10º	41.70º	1600-1900	Turkey	Old growth; possible fire	MB2016
KAA	ABNO	18/9	41.46º	42.11º	1750	Turkey	Managed forest	MB2016
KINH	FAOR	23/20	41.75º	42.11º	2060	Georgia	Old growth	this work
GOR	FAOR	23/13	41.37º	41.94º	1980	Turkey	Old growth	this work
KAF	FAOR	20/10	41.30º	41.90º	1830-2120	Turkey	Managed forest	KG2013
QPS	FAOR	26/18	41.49º	42.04º	1780	Turkey	Old growth	this work
KINM	FAOR	23/18	41.75º	42.10º	1700	Georgia	Old growth	this work
KEDA	FAOR	17/15	41.61º	41.94º	1100	Georgia	Managed forest	this work
KUR	PCOR	28/17	41.47º	42.14º	2075	Turkey	Recent logging	this work
CAM	PCOR	36/27	41.49º	42.04º	1770-1930	Turkey	Old growth	this work
DUP	PCOR	27/14	41.46º	42.11º	1750	Turkey	Managed forest	MB2016
HAH	PCOR	25/24	41.10º	41.70º	1600-1900	Turkey	Old growth	MB2016
KINM	PCOR	24/14	41.75º	42.10º	1700	Georgia	Old growth	this work
BOR	PCOR	13/13	41.82º	43.29º	1315	Georgia	Secondary forest	this work
HAT	PIPN	14/11	41.21º	41.79º	380	Turkey	Open forest; possible fire	MB2016
TURK009	PISY	13/13	40.33º	42.58º	2600	Turkey	na	ITRDB
DMH	PISY	76/43	41.44º	42.31º	2300-2400	Turkey	Tree line; cattle grazing	this work
IRIK	PISY	46/28	43.28º	42.61º	2300	Russia	Tree line	HO2015
TURK022	PISY	28/na	40.33º	41.98º	2100	Turkey	na	ITRBD
GEOR010	PISY	58/29	41.91º	42.85º	2010	Georgia	na	ITRDB
GEOR006	PISY	33/16	41.62º	42.72º	2000	Georgia	na	ITRDB
GEOR003	PISY	49/25	41.72º	43.50º	1950	Georgia	na	ITRDB
GEOR009	PISY	28/14	41.58º	42.75º	1900	Georgia	na	ITRDB
GEOR002	PISY	64/29	41.72º	43.48º	1850	Georgia	na	ITRDB
GEOR008	PISY	26/14	41.77º	43.52º	1850	Georgia	na	ITRDB
GEOR004	PISY	50/24	41.78º	43.48º	1450	Georgia	na	ITRDB
GEOR005	PISY	59/29	41.80º	43.45º	1100	Georgia	na	ITRDB
BOR	QUPE	33/23	41.83º	43.30º	1323	Georgia	Managed forest	this work
MUR	QUPE	42/25	41.33º	41.61º	913	Turkey	Old growth	MB2016
CUB	QUPE	33/15	41.31º	41.59º	650	Turkey	Old growth	MB2016
KUT	QURO	10/9	42.16º	42.76º	200	Georgia	Managed forest	this work
AJA	ZECA	13/6	42.17º	42.76º	200	Georgia	Managed forest	this work

Species codes are: ABNO (*Abies nordmanniana*), FAOR (*Fagus orientalis*), PCOR (*Picea orientalis*), PIPN (*Pinus pinea*), PISY (*Pinus sylvestris*), QUPE (*Quercus petraea*), QURO (*Quercus robur*), ZECA (*Zelkova carpinifolia*). na, information not available.

a, Sources: HO2015 (Holobâcă, Pop & Petrea, 2016); KG2013 (Köse & Güner, 2012); MB2016 (Martin-Benito et al., 2016); ITRDB, International Tree-Ring Data Bank (www.ncdc.noaa.gov/data-access/paleoclimatology-data/datasets/tree-ring). For ITRDB chronologies, site code corresponds to ITRDB accession code.

Supplementary results

Table S3. Summary statistics of all chronologies in the network

Site code	Species	Time span	Length in years: Mean (range)	Rbar[a]	EPS>0.85[b]
KUR	ABNO	1662-2014	201 (89-353)	0.599	1730
SAH	ABNO	1670-2014	155 (47-282)	0.588	1730
GEOR007	ABNO	1676-2006	138 (61-330)	0.579	1820
HAH	ABNO	1667-2013	227 (86-323)	0.564	1745
KAA	ABNO	1600-2007	211 (151-408)	0.666	1625
KINH	FAOR	1618-2014	168 (90-285)	0.576	1770
GOR	FAOR	1540-2013	220 (111-470)	0.687	1725
KAF	FAOR	1559-2008	287 (173-449)	0.701	1660
QPS	FAOR	1549-2013	266 (90-465)	0.678	1650
KINM	FAOR	1668-2014	197 (99-347)	0.616	1745
KEDA	FAOR	1671-2014	201 (121-339)	0.574	1860
KUR	PCOR	1596-2014	251 (165-419)	0.651	1700
CAM	PCOR	1588-2014	224 (91-427)	0.508	1790
DUP	PCOR	1498-2007	348 (121-500)	0.615	1610
HAH	PCOR	1693-2013	215 (80-319)	0.576	1750
KINM	PCOR	1697-2014	203 (95-318)	0.552	1775
BOR	PCOR	1815-2014	136 (99-200)	0.546	1745
HAT	PIPN	1773-2011	163 (80-239)	0.71	1830
TURK009	PISY	1690-1992	203 (143-303)	0.501	1840
DMH	PISY	1613-2014	238 (94-402)	0.57	1745
IRIK	PISY	1810-2009	132 (79-200)	0.617	1870
TURK022	PISY	1717-2001	163 (93-265)	0.548	1810
GEOR010	PISY	1813-2006	111 (53-193)	0.573	1860
GEOR006	PISY	1833-2006	112 (27-171)	0.545	1890
GEOR003	PISY	1781-2006	145 (43-226)	0.6	1840
GEOR009	PISY	1882-2006	99 (38-125)	0.535	1900
GEOR002	PISY	1754-2006	153 (31-253)	0.597	1810
GEOR008	PISY	1767-2006	147 (65-240)	0.526	1820
GEOR004	PISY	1776-2006	147 (70-231)	0.62	1830
GEOR005	PISY	1773-2006	147 (63-234)	0.621	1830
BOR	QUPE	1562-2014	179 (52-453)	0.519	1745
MUR	QUPE	1748-2013	185 (84-266)	0.521	1800
CUB	QUPE	1639-2013	173 (38-272)	0.558	1750
KUT	QURO	1872-2013	107 (64-140)	0.582	1900
AJA	ZECA	1857-2012	118 (64-156)	0.574	1900

a, Rbar: mean interseries correlation. b, year after which the expressed population signal (EPS) is above the common used threshold of 0.85 (Wigley, Briffa & Jones, 1984). Site and species codes as in Table S2.

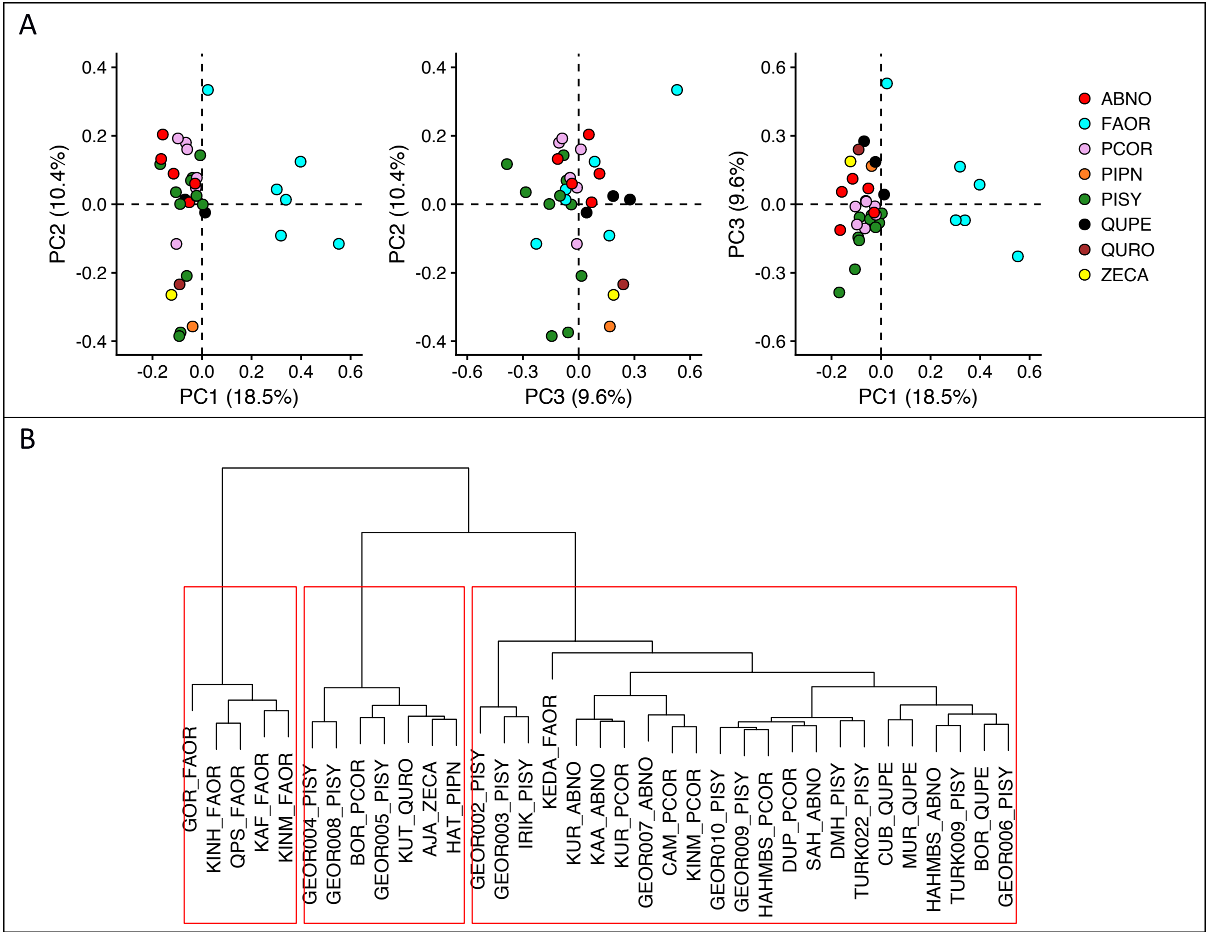

Figure S4.

A, loadings for the first three principal components based on the PCA for the common period 1900-1992. Percentage of variance explained by each principal component is shown in parenthesis. Bottom panel shows the resulting clusters of sites from hierarchical cluster analysis based on PCA results. Site and species codes as in Table S2.

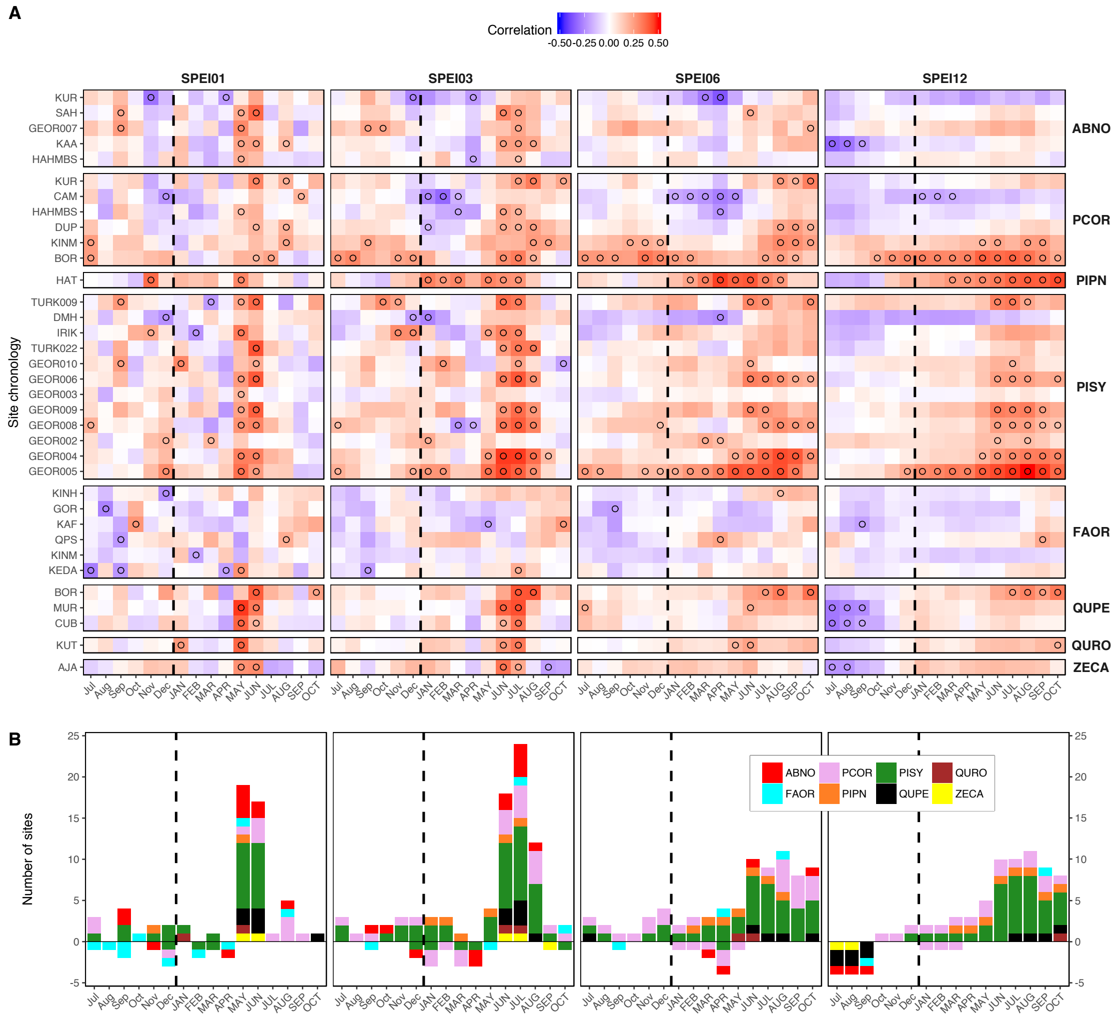

Figure S5. Correlation coefficients for standardized precipitation evapotranspiration index (SPEI) between previous year July (Jul) and current October (OCT) for the time scales of 1, 3, 6 and 12 months between 1930 and 2009 or to the end of each series. Empty circles and black dots signal coefficients that are significant at p ≤ 0.05 and at p ≤ 0.1, respectively. Within each species, sites are ordered in decreasing elevation from top to bottom. Bottom panel (B) summarizes the number of sites with significant correlations (p<0.05) per month. Site and species codes as in Table S2.

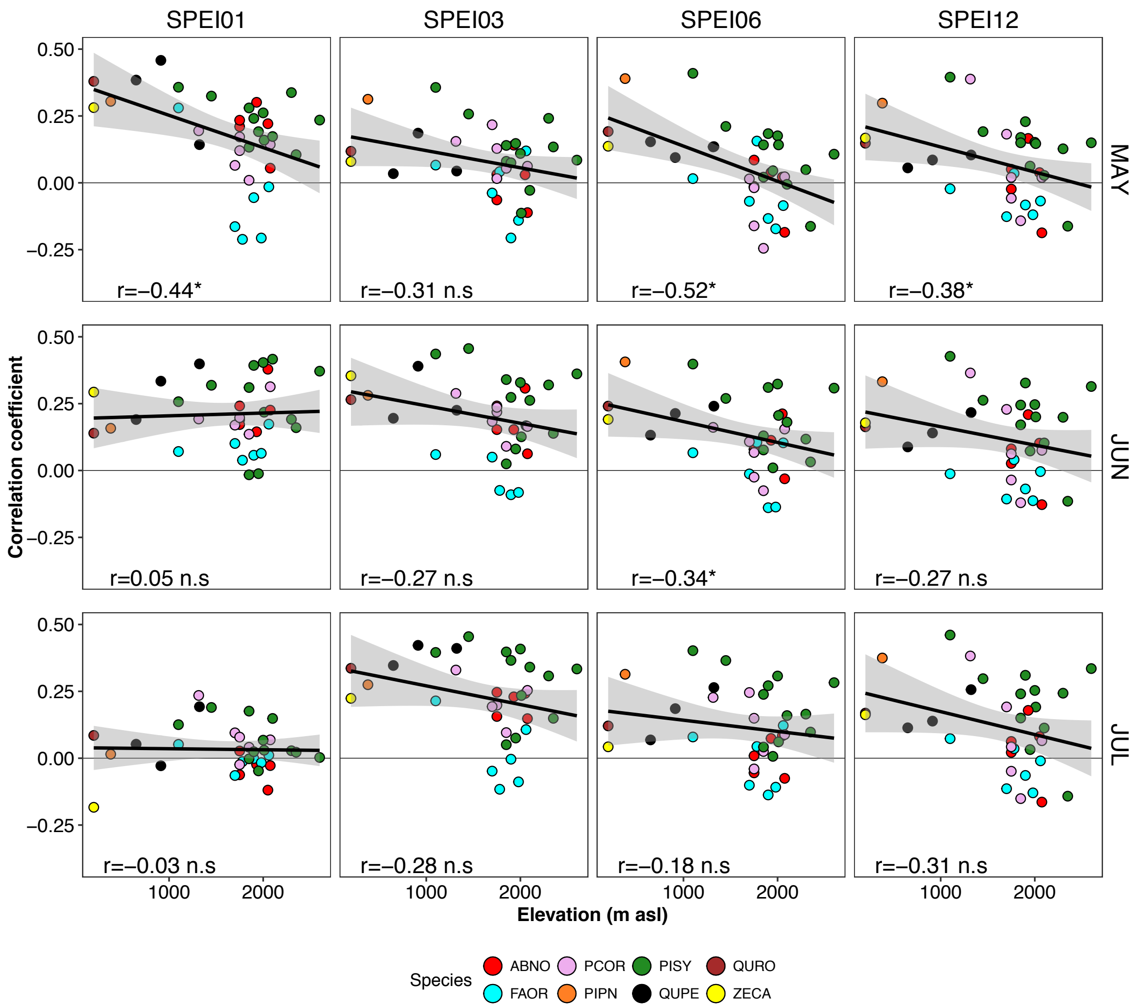

Figure S6. Monthly SPEI correlations at different time scales as a function of elevation. Linear models are fitted to the 35 sites independent of species. (*) denote significant correlations at p ≤ 0.05; n.s. are not significant effects. Grey shades represent 95% confidence intervals. Site and species codes as in Table S2.

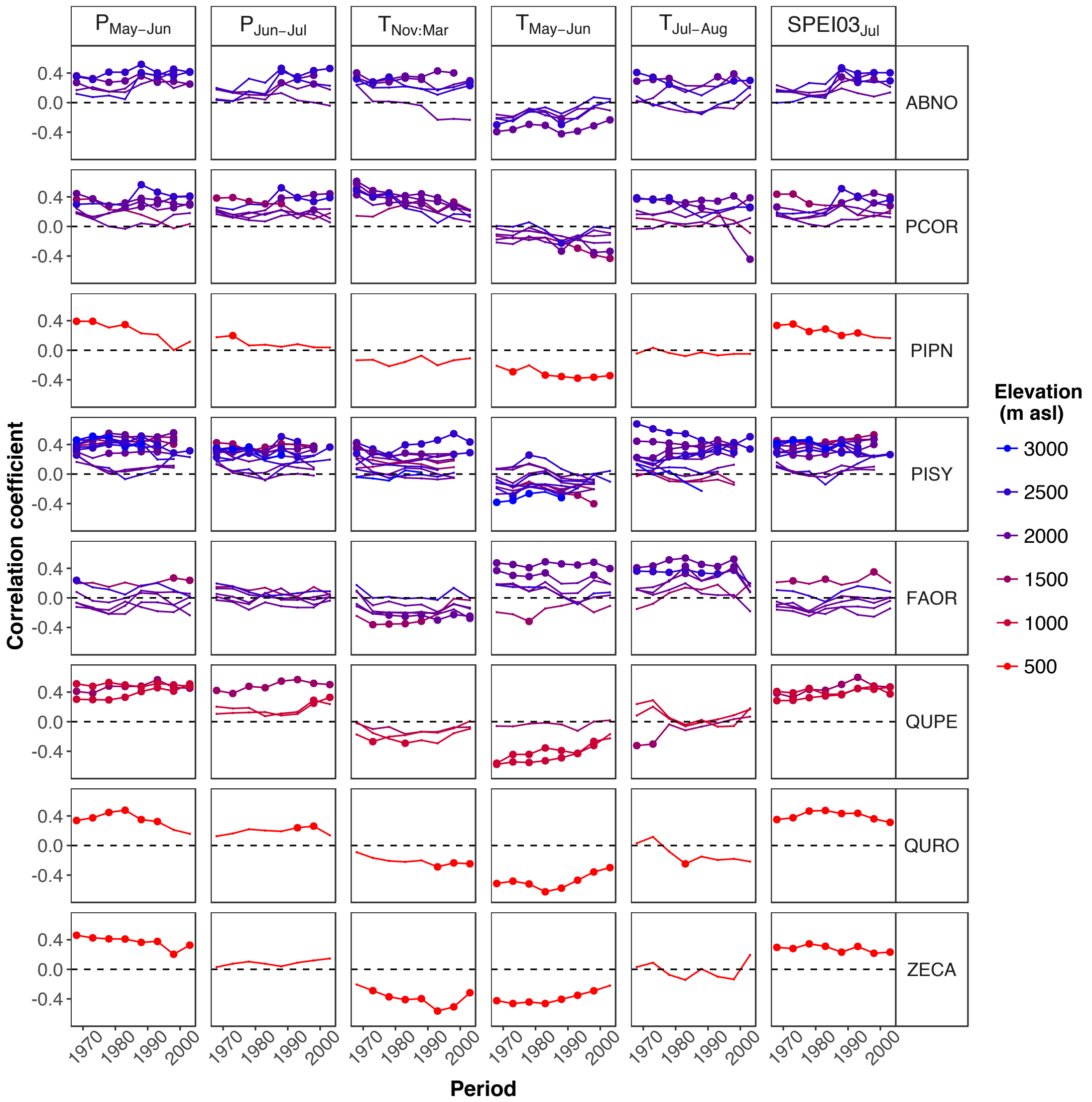

Figure S7. Moving correlation coefficients between growth indices and climate with 40 year windows and 5-year offsets for each site and species. Dots represent coefficients significant at $p \leq 0.05$. Site and species codes as in Table S2.

Supplementary references

Browicz, K. (1989) Chorology of the Euxinian and Hyrcanian element in the woody flora of Asia. *Woody plants—evolution and distribution since the Tertiary*, pp 305-314. Springer.

Cullen, H. M. & Demenocal, P. B. (2000) North Atlantic influence on Tigris–Euphrates streamflow. *International Journal of Climatology*, **20**, 853-863.

Daniel, R. & Simone, P. (2018) Cryphonectria parasitica, the causal agent of chestnut blight: invasion history, population biology and disease control. *Molecular Plant Pathology*, **19**, 7-20.

Dellasala, D. A. (2011) Rainforests at the Margins: Regional Profiles. *Temperate and Boreal Rainforests of the World: Ecology and Conservation* (ed. by D.A. Dellasala), pp 213-242. Island Press/Center for Resource Economics.

Fleck, S., Niinemets, Ü., Cescatti, A. & Tenhunen, J. D. (2003) Three-dimensional lamina architecture alters light-harvesting efficiency in Fagus: a leaf-scale analysis. *Tree Physiology*, **23**, 577-589.

Golubev, Y. N., Kuftarkov, A. Y. & Golubeva, Z. A. (1993) Seasonal fields of tangenital wind stress over the Black Sea. *Physical Oceanography*, **4**, 323-330.

Harris, I., Jones, P. D., Osborn, T. J. & Lister, D. H. (2014) Updated high-resolution grids of monthly climatic observations - the CRU TS3.10 Dataset. *International Journal of Climatology*, **34**, 623-642.

Holobâcă, I.-H., Pop, O. & Petrea, D. (2016) Dendroclimatic reconstruction of late summer temperatures from upper treeline sites in Greater Caucasus, Russia. *Quaternary International*, **415**, 67-73.

Köse, N. & Güner, H. T. (2012) The effect of temperature and precipitation on the intra-annual radial growth of *Fagus orientalis* Lipsky in Artvin, Turkey. *Turkish Journal of Agriculture and Forestry*, **36**, 501-509.

Kottek, M., Grieser, J., Beck, C., Rudolf, B. & Rubel, F. (2006) World map of the Köppen-Geiger climate classification updated. *Meteorologische Zeitschrift*, **15**, 259-263.

Kozlowski, G. & Gratzfeld, J. (2013) *Zelkova-an ancient tree: global status and conservation action*, edn. Natural History Museum.

Kvavadze, E. V. & Connor, S. E. (2005) *Zelkova carpinifolia* (Pallas) K. Koch in Holocene sediments of Georgia—an indicator of climatic optima. *Review of Palaeobotany and Palynology*, **133**, 69-89.

Martin-Benito, D., Ummenhofer, C. C., Köse, N., Güner, H. T. & Pederson, N. (2016) Tree-ring reconstructed May-June precipitation in the Caucasus since 1752 CE. *Climate Dynamics*, **47**, 3011–3027.

Niinemets, Ü. & Valladares, F. (2006) Tolerance to shade, drought, and waterlogging of temperate northern hemisphere trees and shrubs. *Ecological Monographs*, **76**, 521-547.

Papini, A., Simeone, M. C., Bellarosa, R., Spada, F. & Schirone, B. (2011) Quercus macranthera Fisch. & Mey. ex Hohen. And Quercus iberica M. Bieb.: Taxonomic definition and systematic relationships with European oaks inferred from nuclear internal transcribed spacer (ITS) data. *Plant Biosystems*, **145**, 37-49.

Rudolf, B., Becker, A., Schneider, U., Meyer-Christoffer, A. & Ziese, M. (2011) New GPCC full data reanalysis version 5 provides high-quality gridded monthly precipitation data. *GEWEX News*, **21**, 4-5.

Stanev, E. V. & Rachev, N. H. (1999) Numerical study on the planetary Rossby modes in the Black Sea. *Journal of Marine Systems*, **21**, 283-306.

Tarkhnishvili, D., Gavashelishvili, A. & Mumladze, L. (2012) Palaeoclimatic models help to understand current distribution of Caucasian forest species. *Biological Journal of the Linnean Society*, **105**, 231-248.

Türkeş, M. & Erlat, E. (2003) Precipitation changes and variability in Turkey linked to the North Atlantic oscillation during the period 1930-2000. *International Journal of Climatology*, **23**, 1771-1796.

Vicente-Serrano, S. M., Beguería, S. & López-Moreno, J. I. (2010) A multiscalar drought index sensitive to global warming: the standardized precipitation evapotranspiration index. *Journal of Climate*, **23**, 1696-1718.

Wigley, T. M. L., Briffa, K. R. & Jones, P. D. (1984) On the Average Value of Correlated Time Series, with Applications in Dendroclimatology and Hydrometeorology. *Journal of Applied Meteorology*, **23**, 201–213.

Zazanashvili, N. (1999) On the Colkhic vegetation. *Conference on Recent Shifts in Vegetation Boundaries of Deciduous Forests, Especially Due to General Global Warming* (ed. by F. Klötzli & G.-R. Walther), pp 181-197. Birkhäuser Basel.

Zazanashvili, N., Gagnidze, R. & Nakhutsrishvili, G. (2000) Main types of vegetation zonation on the mountains of the Caucasus. *Acta Phytogeographica Suecica*, **85**, 7-16.

Zveryaev, I. I. (2004) Seasonality in precipitation variability over Europe. *JOURNAL OF GEOPHYSICAL RESEARCH*, **109**.